Development 134, 1745-1754 (2007) doi:10.1242/dev.02840

Protease nexin 1 and its receptor LRP modulate SHH signalling during cerebellar development

Catherine Vaillant[1], Odyssé Michos[2], Slobodanka Orolicki[1], Florence Brellier[1], Sabrina Taieb[1], Eliza Moreno[1], Hélène Té[1], Rolf Zeller[2] and Denis Monard[1,*]

Development of the postnatal cerebellum relies on the tight regulation of cell number by morphogens that control the balance between cell proliferation, survival and differentiation. Here, we analyze the role of the serine-protease inhibitor protease nexin 1 (PN-1; SERPINE2) in the proliferation and differentiation of cerebellar granular neuron precursors (CGNPs) via the modulation of their main mitogenic factor, sonic hedgehog (SHH). Our studies show that PN-1 interacts with low-density lipoprotein receptor-related proteins (LRPs) to antagonize SHH-induced CGNP proliferation and that it inhibits the activity of the SHH transcriptional target GLI1. The binding of PN-1 to LRPs interferes with SHH-induced cyclin D1 expression. CGNPs isolated from *Pn-1*-deficient mice exhibit enhanced basal proliferation rates due to overactivation of the SHH pathway and show higher sensitivity to exogenous SHH. In vivo, the *Pn-1* deficiency alters the expression of SHH target genes. In addition, the onset of CGNP differentiation is delayed, which results in an enlarged outer external granular layer. Furthermore, the *Pn-1* deficiency leads to an overproduction of CGNPs and to enlargement of the internal granular layer in a subset of cerebellar lobes during late development and adulthood. We propose that PN-1 contributes to shaping the cerebellum by promoting cell cycle exit.

KEY WORDS: Protease nexin 1, Sonic hedgehog, Low density lipoprotein, Receptor-related protein (LRP), Proliferation, Cerebellum, Mouse

INTRODUCTION

Protease nexin 1 (PN-1; also known as SERPINE2 – Mouse Genome Informatics) is a 43 kDa member of the serpin superfamily and inhibits serine proteases (Baker et al., 1980; Gloor et al., 1986; Knauer et al., 2000). After secretion, PN-1 is complexed with its target proteases and binds to specific members of the low density lipoprotein receptor-related protein (LRP) family (Strickland and Ranganathan, 2003). The ligands are internalized in endosomes via clathrin-coated pits and are degraded in lysosomes. Simultaneously, the intracellular LRP domain signals, via coupling, to adaptor and scaffold proteins (Schneider and Nimpf, 2003). The role of PN-1 in the adult brain has been studied (Kvajo et al., 2004; Luthi et al., 1997), but possible functions during nervous system development remained elusive. During embryogenesis and in the postnatal brain, *Pn-1* is expressed prominently in areas of high remodelling, in which cell proliferation and fate specification are influenced by morphogens such as sonic hedgehog (SHH) (Kury et al., 1997; Mansuy et al., 1993). SHH is a key regulator of vertebrate morphogenesis (Ingham and McMahon, 2001) and its binding to the patched homolog 1 (PTC1; also known as PTCH1 – Mouse Genome Informatics) receptor causes the cessation of smoothened (SMO)-mediated inhibition of signal transduction and triggers the activation of the GLI family of transcriptional regulators (Ho and Scott, 2002). In the developing CNS, *Shh* and *Pn-1* are co-expressed in the ventral part of the mesencephalon and myelencephalon, and in the mid-hindbrain junction, otic vesicles and cerebellum (Dahmane and Altaba, 1999; Mansuy et al., 1993; Wallace, 1999; Wechsler-Reya and Scott, 1999).

The developing cerebellum is a good model in which to study the regulatory pathways that coordinate cell proliferation with cell survival and differentiation. In rodents, this cortical structure is transiently enveloped by the external granular layer (EGL), which consists of cerebellar granular neuron precursors (CGNPs), which proliferate from birth until postnatal day 15 (P15). SHH is considered as the main proliferative signal of CGNPs (Dahmane and Altaba, 1999; Kenney and Rowitch, 2000; Wallace, 1999; Wechsler-Reya and Scott, 1999), a role that requires the extracellular modulation of SHH by heparan sulfates (Rubin et al., 2002) and the binding of the chemokine SDF-1 (also known as CXCL12 – Mouse Genome Informatics) to its receptor CXCR4 (Klein et al., 2001). By contrast, negative regulators of SHH signalling such as vitronectin (Pons et al., 2001), fibroblast growth factor 2 (FGF2) (Wechsler-Reya and Scott, 1999), BMPs (Rios et al., 2004) and PACAP (also known as ADCYAP1 – Mouse Genome Informatics) (Nicot et al., 2002) induce cell cycle exit and the differentiation of CGNPs.

Our results show that PN-1 modulates the signalling activity of SHH and promotes the differentiation of CGNPs and Bergmann glia. In particular, we establish that PN-1 antagonizes SHH-induced proliferation of CGNPs. In *Pn-1*-deficient mice, the expression of SHH targets is enhanced in the EGL and Bergmann glia, which correlates well with the delayed differentiation of CGNPs and altered maturation of Bergmann glia. In particular, the *Pn-1* deficiency causes an increase in mature granular cells. We conclude that the interaction of PN-1 with SHH is important for shaping the cerebellum during its postnatal development.

MATERIALS AND METHODS

Materials

The 19 kDa N-terminal fragment of SHH was kindly provided by S. Pons [Instituto de Biologia Molecular de Barcelona (CSIC), Barcelona, Spain] and U. Mueller (Scripps Institute, San Diego, CA, USA), or from R&D Systems. FGF2 was purchased from R&D Systems, and KAAD-cyclopamine from Invitrogen. Rat recombinant PN-1 was purified and the P960 and P965 peptides produced as described previously (Knauer et al.,

[1]Friedrich Miescher Institute for Biomedical Research, Maulbeerstrasse 66, 4058-CH Basel, Switzerland. [2]Developmental Genetics, DKBW Centre for Biomedicine, University of Basel Medical School, Basel, Switzerland.

*Author for correspondence (e-mail: denis.monard@fmi.ch)

Accepted 21 February 2007

1997a; Sommer et al., 1989). RAP (also known as LRPAP1 – Mouse Genome Informatics) was a generous gift from M. Etzerodt (University of Aarhus, Aarhus, Denmark).

Mice

Wild-type C57BL6/J mice were purchased from Charles River (France). Homozygous *Pn-1* knockout (Luthi et al., 1997) and knock-in (Kvajo et al., 2004) mice were backcrossed in the C57BL6/J line for 11 generations. Heterozygous matings of *Pn-1*-deficient mice allowed the comparative analysis of littermates of all genotypes. All animal experiments were performed according to the Swiss laws governing animal experimentation and approved by the Swiss veterinary authorities.

Primary cultures of CGNPs

CGNPs were isolated from P5-P8 mice cerebella over a Percoll gradient, as described previously (Hatten et al., 1988). Purified CGNPs were re-suspended in 10% horse-serum medium and 10^6 cells per well were plated in 24 well plates on glass coverslips coated with poly-L-lysine (10 or 500 μg/ml; Fluka). After overnight recovery, cells were cultured in serum-free medium containing 1% stripped BSA and I-1884 supplement (Sigma). Depending on the assay, the culture medium was supplemented with either 50, 100, 200 or 3000 ng/ml SHH, and/or 30 or 210 nM PN-1, and/or 1 μg/ml RAP for 48 hours. Bergmann glial cells were isolated and purified as described previously (Hatten, 1985). For proliferation studies, cells were incubated with 10 μg/ml BrdU for 16 hours. Mixed cultures from *Pn-1*-deficient mice were prepared from individually processed cerebella to compare proliferation rates among age-matched littermates. All coverslips were processed for BrdU immunostaining and were counterstained with Hoechst. Pictures were acquired using a Leica DMR microscope and a SPOT-1 digital camera. Fluorescent staining was analyzed using Image-Pro Plus (Media Cybernetics). For proliferation index determination, the ratio of BrdU-positive cells/Hoechst-labelled cells was calculated over ten fields per coverslip. The averages were calculated using four independent experiments.

Beta-galactosidase staining and activity assays

Beta-galactosidase-detection and -activity assays were performed as described previously (Kvajo et al., 2004). CGNPs were incubated overnight in serum-free medium with or without FGF2 (25 or 50 ng/ml) and/or SHH (3 μg/ml), lysed and processed using the Galacto-Star kit (Applied Biosystems), and analyzed using a microplate reader.

Immunohistochemistry and immunocytochemistry

Cells grown on coverslips were post-fixed in 4% paraformaldehyde and the antibodies used were: anti-beta-III-tubulin (1/200, Chemicon), 4B3 monoclonal anti-PN-1 (1/100) (Meier et al., 1989), anti-LRP1 (1/200; provided by D. Strickland, Department of Biochemistry, American Red Cross, MD, USA), anti-prominin 1 (1/300, Chemicon), anti-GFAP (1/500, Sigma). P10 wild-type and *Pn-1*-knockout mice were injected intraperitoneally with BrdU (Sigma) at 100 μg/g of body weight, and brains isolated 1 hour later. Cryostat or paraffin sections (12 μm and 6 μm, respectively) were stained using: anti-PN-1 (1/100), anti-LRP1 (1/100), anti-calbindin-28K (1/200, Sigma), anti-BrdU (1/250, BD Pharmingen), anti-GFAP (1/1000, Sigma), anti-p27 (1/100, BD Pharmingen), anti-MATH1 (also known as anti-ATOH1; 1/100; generous gift from J. Johnson, University of Texas Southwestern Medical Center, Dallas, TX, USA) and anti-doublecortin (1/100, Santa Cruz Biotechnology). The specificity of the PN-1 antiserum was established by the absence of staining in cerebella of *Pn-1*-deficient mice (data not shown). Alexa Fluor 488 or horseradish peroxidase (HRP)-coupled antibodies included anti-mouse (1/500, Molecular Probes; 1/1000, Amersham Bioscience) and anti-rabbit (1/500, Molecular Probes). PN-1, LRP1 and doublecortin immunostainings were performed using a Discovery XT automated stainer (Ventana Medical Systems) with Ventana DAB Map detection kit (Easwaran et al., 2003). Antigen retrieval was achieved in CC1 and CC2 buffers (Ventana). Secondary biotinylated antibodies were: donkey anti-goat (1/200, Jackson ImmunoResearch) and Ventana universal secondary antibody. Signals were amplified using the AmpMap kit with TSA (Ventana). Sections from wild-type and mutant mice were processed simultaneously. Quantification of BrdU labelling and p27-positive cells was performed on mid-sagittal sections in the region of the pre-culminate fissure of lobes III and IV. The average ratio of BrdU- or p27-positive to -negative CGNPs was determined over 200 μm of EGL for each cerebellum.

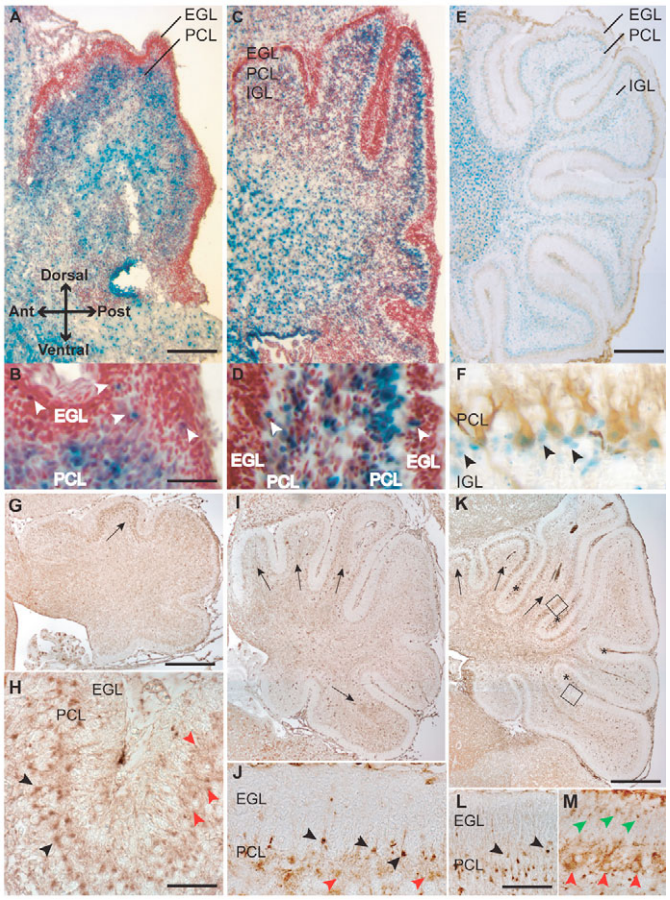

Fig. 1. Distribution of *Pn-1*-expressing cells and the PN-1 protein during cerebellar development. PN-1 expression was monitored by beta-galactosidase detection in the developing postnatal cerebellum of PN-1 knock-in mice (**A-F**) and the distribution of the PN-1 protein was determined using specific antibodies (**G-M**). Following beta-galactosidase detection, sagittal sections were counterstained with neutral red (A-D) or anti-calbindin (E,F) to identify Purkinje cells and Bergmann glia. At early stages [P0 (A,B) and P2 (C,D)] beta-galactosidase activity is detected in Purkinje cells and in some CGNPs (arrowheads). By P8 (E,F), the overall expression is reduced and the labelling of the EGL has vanished. Beta-galactosidase activity remains in Purkinje cells and in the surrounding Bergmann glia cell bodies (F, arrowheads). At P0 (G,H), P2 (I,J) and P8 (K,M), the PN-1 protein is detected in the PCL. High levels of PN-1 protein are observed in the Bergmann glial cells (H,J,L, black arrowheads) and diffuse staining is observed in Purkinje cell bodies and dendrites (H,J,M, red arrowheads). Some PN-1 protein is also detected in postmitotic CGNPs (M, green arrowheads). The PN-1-protein distribution is graded along the anteroposterior axis. Initially (P0), it is rather prominent in the dorsal anterior lobes (G, arrow), and it then (P2) extends to the dorsal anterior and ventral posterior lobes (I, arrows). Later (P8), PN-1 protein is present in the dorsal anterior lobes (K, arrows) and in the deep fissures of the central lobes (K, asterisks). EGL, external granular layer; IGL, internal granular layer; PCL, Purkinje cell layer. Scale bars: 200 μm in A for A,C and in G for G,I; 50 μm in B for B,D,F; 250 μm in E; 30 μm in H for H,J; 350 μm in K; 60 μm in L for L,M.

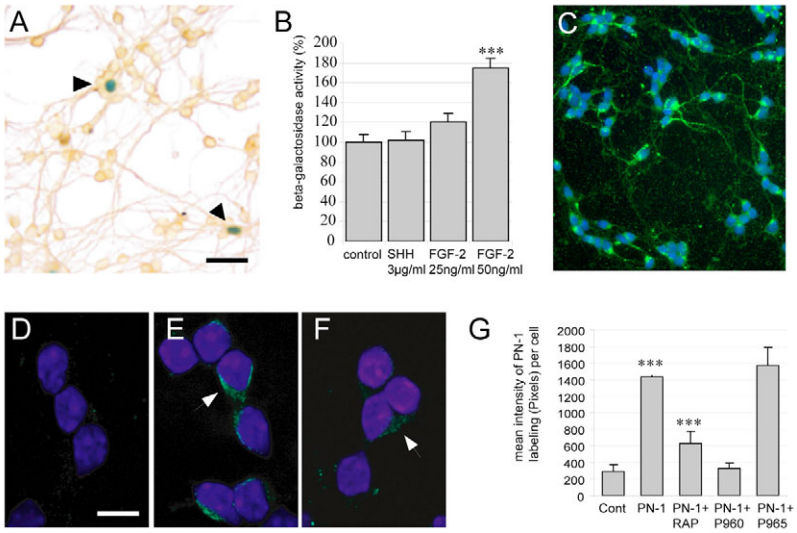

Fig. 2. PN-1 is internalized via LRP1-mediated endocytosis by all cultured CGNPs. CGNPs from *Pn-1* knock-in mice (P8) were cultured for 48 hours on polylysine substrate (500 μg/ml). (**A**) *Pn-1*-expressing cells (counterstained by anti-beta-III tubulin in brown) were identified by beta-galactosidase activity (arrowheads). (**B**) SHH and FGF2 were tested for their ability to stimulate *Pn-1* expression in cultured CGNPs from *Pn-1* knock-in mice (P5). FGF2 markedly increases *Pn-1* expression, whereas SHH does not. (**C**) LRP1 immunodetection (green) indicates that this receptor is present in/on the cell body and processes of all cells. (**D-G**) Uptake of recombinant PN-1 is antagonized by blocking LRP1-binding sites. PN-1 immunodetection was performed on CGNPs (P8) incubated for 4 hours with control medium (D), or with medium supplemented with 60 nM PN-1 (E), with 60 nM PN-1 plus 1 μg/ml RAP (F), or with 25 μg/ml P960 or P965 (not shown). Arrowheads show PN-1-containing CGNPs. (G) Quantitation of the mean PN-1 immunolabelling per cell. Values are expressed as mean±s.e.m. (***P<0.001; Student's t-test). Scale bars: 20 μm in A for A,C; 5 μm in D for D-F.

In situ hybridization

In situ hybridizations were performed using 6 μm sagittal brain sections and *Gli1*, *Gli3*, *Shh* and *Ptc1* RNA probes as described previously (Michos et al., 2004).

Semi-quantitative RT-PCR analysis

Total RNA was extracted from cultured CGNPs or dissociated cerebellar cells using the RNeasy kit (Qiagen). First-strand cDNAs were synthesized using AMV Reverse Transcriptase (Promega). A total of 2 μl of each cDNA sample was used for PCR amplification of the *Shh*, *Ptc1*, *Gli1* and *Gli3* transcripts. Beta-actin was used to normalize samples (primer sequences and PCR conditions are available on request).

Western blotting

CGNP cultures and cerebella were homogenized in NP-40 lysis buffer. Proteins (20 μg) were subjected to 10% SDS-PAGE and transferred to a nitrocellulose membrane (Bio-Rad Laboratories). Antibodies were: anti-cyclin D1 (clone 72-13G; 1/1000, Santa-Cruz Biotechnology), anti-cyclin D2 (clone 34B1-3; 1/300, Santa-Cruz Biotechnology) and anti-actin (1/3000, NeoMarkers). Secondary HRP-conjugated antibodies were anti-mouse (1/5000, Amersham Bioscience) and anti-goat (1/2000, Jackson ImmunoResearch). Blots were developed using enzymatic chemiluminescence (ECL) (Amersham Bioscience) and were quantified with ImageMaster total lab v2.00.

PN-1 uptake studies

CGNPs from P8 mice were cultured for 24 hours, pre-cultured in serum-free medium for 2 hours and supplemented with lysosome inhibitors for 1 hour, all at 37°C (leupeptin, 10 μg/ml; pepstatin A, 20 μM). Recombinant PN-1 (60 nM) was then added with or without RAP (1 μg/ml), P960 (25 μg/ml) and/or P965 (25 μg/ml) and incubated for 4 hours at 37°C. Cells were washed, stained using anti-PN-1 (1/800) and Alexa Fluor 488-coupled anti-mouse antibodies (1/500, Molecular Probes). Hoechst-counterstained cells were analyzed using a Zeiss LSM510 confocal microscope. For quantification, five randomly chosen pictures were taken for each sample in each experiment and analyzed using Image-Pro Plus.

GLI activity reporter assay

NIH3T3 cells were transiently co-transfected with 6 μg of the CAT reporter plasmid pA10CAT6GBS [containing multiple GLI-binding sites (Dai et al., 1999); provided by S. Ishii, RIKEN Tsukuba Institute, Ibaraki, Japan] and 1 μg of beta-galactosidase reporter plasmid. After 24 hours, 3 μg/ml SHH and/or 30 nM PN-1 were added during 24 hours in serum-free medium supplemented with 1% stripped BSA. After lysis, 100 μg of proteins were used to determine CAT activity (CAT ELISA system; Roche).

Morphological quantitation of granular layers and 3-D reconstruction

The thicknesses of the EGL and internal granular layer (IGL) were quantified on sagittal medial sections of wild-type and mutant cerebella at P10 and in adults. The maximal width of the EGL and IGL in lobes VI (L1) and VIII (L2) was measured and averaged over four adjacent sections using Image-Pro Plus. Data were analyzed using a two-way ANOVA test (n=4 for P10 animals; n=5 for adults; Graphpad Prism). For 3-D reconstructions, 6 μm sagittal paraffin sections of P10 and adult cerebella were stained with cresyl violet at intervals of 60 μm, and digital pictures of all serial sections were aligned and reconstructed using ImageAccess, AutoAligner2 and Imaris 5.0.3 (Bitplane).

RESULTS

Expression and distribution of the *Pn-1* gene products in the developing postnatal cerebellar cortex

The distribution of PN-1-producing cells was determined using reporter mice with nuclear beta-galactosidase activity to identify *Pn-1* expression (Kvajo et al., 2004) and the PN-1 protein was detected using specific antibodies. At birth (P0), beta-galactosidase activity was detected in cells of the inner mass of the cerebellum, corresponding to migrating Purkinje and glial cells (Fig. 1A,B). A few *Pn-1*-expressing cells were also detected in the EGL overlaying the cerebellum, possibly corresponding to precursors (Fig. 1B, arrowheads).

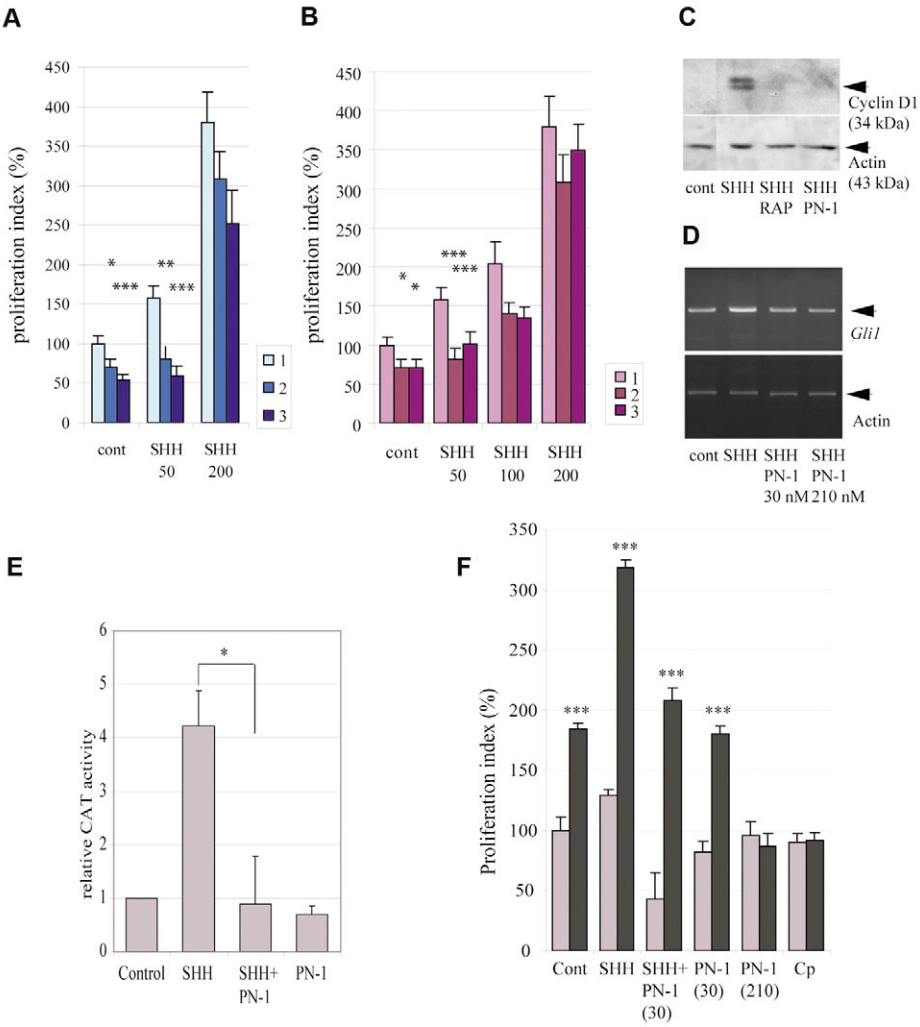

Fig. 3. PN-1 negatively modulates SHH signal transduction in CGNPs. (**A**,**B**) CGNPs of P5 wild-type mice cerebella were cultured on polylysine (10 μg/ml) for 48 hours alone or with recombinant SHH and recombinant PN-1, and were then pulsed with BrdU for 16 hours. (A) The ratio of BrdU-positive cells/total number of CGNPs was determined and the proliferation index normalized with respect to the control value, which was set at 100% (corresponding to 1.4% BrdU-positive CGNPs). Addition of 50 or 200 ng/ml SHH stimulates BrdU incorporation (series 1). Addition of 30 nM (series 2) or 210 nM (series 3) PN-1 together with SHH significantly inhibits the stimulation of cell proliferation. Notice that the addition of PN-1 alone inhibits proliferation in comparison to the control. Error bars indicate s.e.m. (**P*<0.05; ***P*<0.01; ****P*<0.001; Student's *t*-test). (B) CGNPs were treated for 48 hours with SHH alone (50, 100 or 200 ng/ml; series 1), together with 30 nM PN-1 (series 2) or SHH, which was added 5 hours prior to 30 nM PN-1 (series 3). Prior addition of SHH does not significantly alter the inhibitory effect of PN-1. (**C**) Following 48 hours of treatment on polylysine substrate (500 μg/ml), CGNPs were lysed and cyclin D1 expression levels were determined. Notice that cyclin D1 protein levels increase in the presence of 3 μg/ml SHH. This increase is inhibited by the addition of 30 nM PN-1 or 1 μg/ml RAP. (**D**) SHH signal transduction was investigated by RT-PCR analysis of *Gli1* expression in CGNPs cultured for 48 hours on a proliferation-permissive substrate (polylysine; 10 μg/ml) in presence of SHH (50 ng/ml) alone or with PN-1 (30 or 210 nM). The addition of SHH increases *Gli1* transcription, which can also be reversed by adding PN-1. (**E**) The antagonistic effect of PN-1 on SHH signal transduction was further studied using co-transfection assays in NIH3T3 cells. A CAT reporter plasmid containing GLI-binding sites and a beta-galactosidase expression plasmid were co-transfected into cells, and, 24 hours later, 3 μg/ml SHH and 30 nM PN-1 were added. A CAT ELISA assay was performed on 100 μg of cell extract prepared after 48 hours. The addition of SHH stimulates the transcriptional activity more than fourfold. This effect is blocked by PN-1. PN-1 alone has no effect. Values represent the mean relative activity of the CAT reporter enzyme after adjustment for transfection efficiency and normalization with mock-transfected controls. (**P*<0.05, Student's *t*-test). (**F**) Inactivation of the *Pn-1* gene enhances the proliferation rates of CGNPs. Mixed cultures of P5 wild-type (grey bars) and *Pn-1*$^{-/-}$ cerebellar cells (black bars) were treated for 48 hours with 3 μg/ml SHH, 30 nM PN-1 (PN-1 30), 210 nM PN-1 (PN-1 210) or KAAD-cyclopamine 1 μg/ml (Cp). The proliferation rates of the CGNPs were determined and results normalized to wild type (*Pn-1*$^{+/+}$ controls). The proliferation rates are expressed as percentages (100% corresponding to 2.98% of BrdU-positive CGNPs). Values shown represent mean±s.e.m. (****P*<0.0001; two-ways ANOVA test). CGNPs from *Pn-1*$^{-/-}$ mice display enhanced proliferation and increased sensitivity to SHH. The proliferation rates are reduced to wild-type levels by adding a high concentration of PN-1 or by blocking SHH signal transduction with KAAD-cyclopamine.

Furthermore, the PN-1 protein was detected in cells of the forming Purkinje cell layer (PCL; Fig. 1G,H, red arrowheads), in Bergmann glial cells (Fig. 1H, black arrowheads), diffusely in the EGL (Fig. 1H) and in the dorsal anterior lobes (Fig. 1G, arrow). By P2, abundant *Pn-1*-expressing cells were detected in the PCL (Fig. 1C,D). The distribution of beta-galactosidase-positive cells was graded along the

anteroposterior axis, being absent or weak in dorsal and ventral parts, but stronger in central lobes. Each of the positive lobes displayed lower beta-galactosidase activity in its invaginations (Fig. 1C). By contrast, the PN-1 protein was rather lower in central than in dorsal and ventral regions (Fig. 1I,J). These regional differences in PN-1 transcript and protein distributions could be due to secretion and internalization of the PN-1 protein by target cells (see below) and/or to additional post-transcriptional regulation. PN-1 distribution within the PCL is rather reminiscent of those of *Shh* and *Gli1* transcripts at equivalent stages (Corrales et al., 2004; Lewis et al., 2004). In the EGL, a few PN-1-positive CGNPs were still scattered throughout the lobes (Fig. 1D, arrowheads). By P8, the overall level of beta-galactosidase activity had decreased (Fig. 1E), but remained in Purkinje and Bergmann glia cell bodies (Fig. 1F, arrowheads). PN-1 protein was detected in dorsal lobes and their invaginations (Fig. 1K, arrows), in Bergmann glia (Fig. 1L, arrowheads), in the PCL and in scattered progenitors of the EGL (Fig. 1M, red and green arrowheads). In adults, *Pn-1* expression was weak and rather homogeneous within the PCL (data not shown). The distribution of the major PN-1 receptor, LRP1, was rather ubiquitous, although was higher in the PCL of the dorsal and ventral regions (similar to PN-1, for details see Fig. S1 in the supplementary material).

Pn-1 is expressed by a subpopulation of cultured CGNPs and is internalized in an LRP1-dependent manner

To further analyze *Pn-1* expression and function, primary cerebellar cells were isolated from P5 reporter mice, cultured for 3 days, and characterized with respect to *Pn-1* expression and their differentiation status (Fig. 2A and see Fig. S2 in the supplementary material). Less than 5% of all cells expressed *Pn-1* (Fig. 2A). Approximately 70% of all PN-1-positive cells corresponded to GFAP-positive astroglia (see Fig. S2 in the supplementary material), which accounted for about 30% of all astrogial cells in the cerebellum. In addition, around 75% of all cerebellar stem cells (positive for prominin 1) (Lee et al., 2005) were PN-1 positive, whereas only few neuronal cell types expressed PN-1 (<3%; data not shown). FGF2 is known to antagonize SHH-mediated proliferation of cultured CGNPs (Wechsler-Reya and Scott, 1999). Interestingly, *Pn-1* expression is upregulated by FGF2 in mid-/hind-brain-derived mesenchymal cells (Kury et al., 1997). To determine whether PN-1 could be a target of SHH and/or FGF2 signal transduction, CGNPs from P5 reporter mice were cultured overnight in medium supplemented with either recombinant SHH or recombinant FGF2 (Fig. 2B). *Pn-1* expression levels were elevated in a dose-dependent manner upon FGF2 addition (Fig. 2B). In particular, FGF2 induced a 30-70% increase in *Pn-1*-expressing astroglial cells (see Fig. S2 in the supplementary material).

Free or complexed extracellular PN-1 binds to LRP1, which mediates its internalization (Knauer et al., 1997b). LRP1 was detected in the cell body and along neurites of all CGNPs (Fig. 2C) and receptor-associated protein (RAP; also known as LRPAP1 – Mouse Genome Informatics)-mediated blocking of LRPs significantly inhibited PN-1 internalization into CGNPs (Fig. 2D-G). Because RAP has a high affinity for all LRPs (Herz et al., 1991), we used the 12 amino acid P960 peptide derived from the N-terminal region of PN-1 to characterize the involved LRP subtype further. This peptide has been shown to specifically interfere with LRP1-mediated PN-1 uptake (Knauer et al., 1997a). Indeed, P960 completely blocked the internalization of recombinant PN-1 (Fig. 2G), which indicates that LRP1 is required for PN-1 internalization by CGNPs.

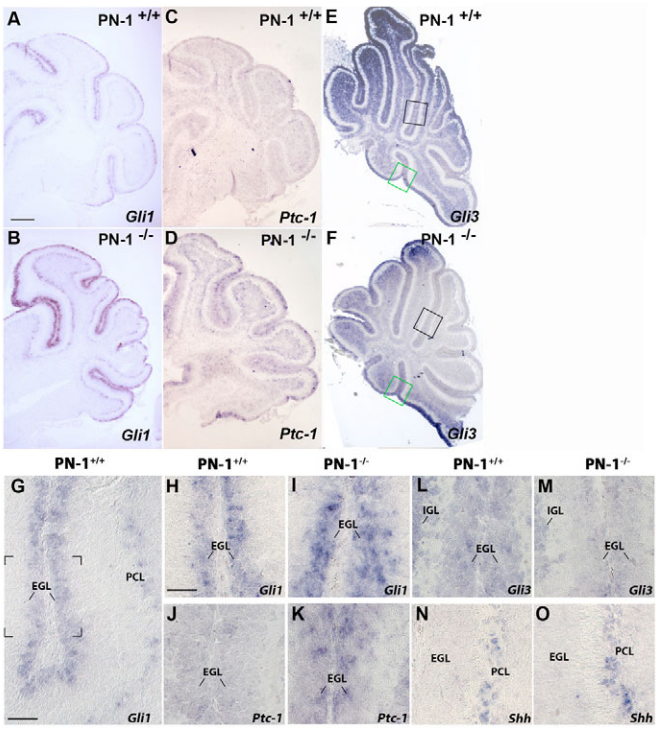

Fig. 4. The expression of SHH target genes is altered in the cerebellum of *Pn-1-deficient* mice. The distribution of *Gli1*, *Patched 1* (*Ptc1*), *Gli3* and *Shh* transcripts were examined in the cerebellum of P8 *Pn-1*$^{+/+}$ and *Pn-1*$^{-/-}$ mice by in situ hybridization. Sagittal sections are shown for each gene at low (**A-F**) and high magnifications (**G-O**). The frame in G indicates the enlargements shown in H-O. The black frames in E,F indicate the enlargements shown in L,M. (A,G,H) *Gli1* is expressed in the EGL and in the Bergmann glia of wild-type mice. (B,I) *Gli1* expression is increased in the EGL of mutants and numbers of expressing precursors are expanded. (C,J) Wild-type *Ptc1* expression. (D,K) *Pn-1* deficiency induces an increase in *Ptc1* expression levels and in the number of *Ptc1*-expressing precursors in the EGL. (E,L) Wild-type *Gli3* expression. (F,M) *Gli3* expression is decreased in the deeper regions of the lobes and within the EGL of mutant mice. The green frames in E,F outline zones of equal expression in both wild type and mutant. (N) *Shh* is predominantly expressed in the PCL of wild-type mice, and is unchanged in mutants (O). At least three independent cerebella were analysed for all genes shown and yielded identical results. EGL, external granular layer; IGL, internal granular layer; PCL, Purkinje cell layer. Scale bars: 250 μm in A for A,F; 30 μm in G; 20 μm in H for H-O.

PN-1 antagonizes SHH signalling in cultured CGNPs

In order to investigate the potential effects of PN-1 on SHH-induced cell proliferation, CGNPs were cultured for 48 hours in the presence of SHH and/or PN-1. Proliferating cells were labelled with BrdU during the last 16 hours to determine their proliferation rates (Fig. 3A,B). As previously reported (Wechsler-Reya and Scott, 1999), the addition of recombinant SHH stimulated CGNP proliferation (Fig. 3A,B, series 1). Such SHH-induced cell proliferation was significantly antagonized by PN-1 using SHH at 50 or 100 ng/ml (Fig. 3A,B, series 2 and 3). Higher SHH concentrations were able to overcome the inhibitory effect of PN-1, which is indicative of its limited modulation potential and/or saturation of the system. To determine whether the antagonistic effect of PN-1 is mediated by receptor competition or via an independent intracellular pathway,

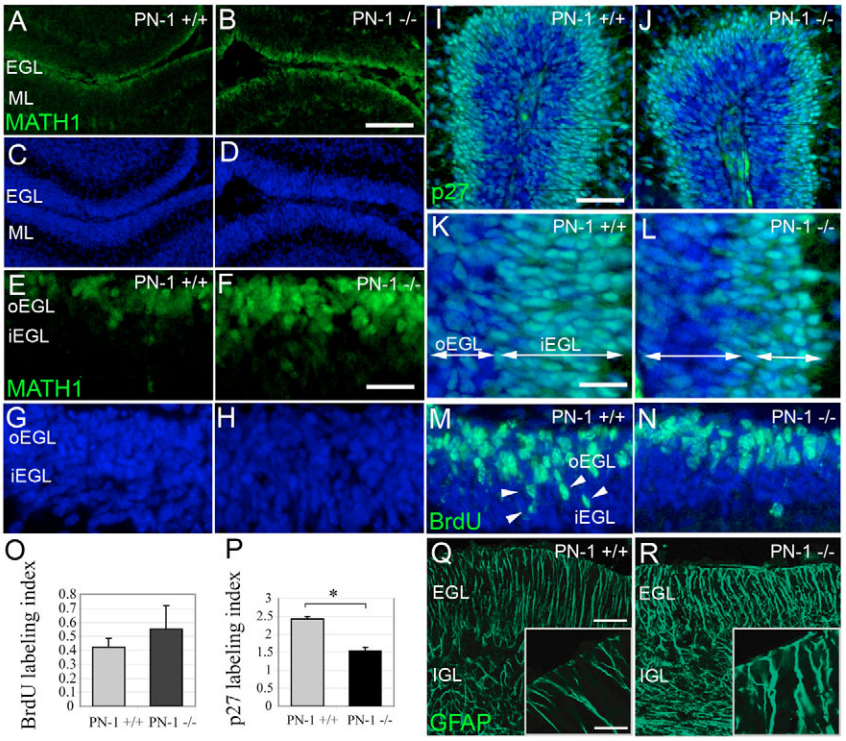

Fig. 5. The *Pn-1* gene deficiency delays the onset of CGNP differentiation in the EGL. (**A-H**) Sections from P10 wild-type (A,C,E,G) and *Pn-1*-deficient mice (B,D,F,H) were immunostained for MATH1 (green; Hoechst, blue). In both groups, MATH1 staining is detected in the oEGL. The zone of MATH1-positive cells is enlarged in *Pn-1*-deficient mice. In addition, the intensity of the MATH1 staining increases at the cellular level. (**I-L**) Sections from P10 wild-type and *Pn-1*-deficient mice were immunostained for p27 (green; Hoechst, dark blue; overlap, light blue). The wild-type EGL is divided into two zones: the oEGL, with few p27-expressing cells, and the iEGL, expressing p27 at high levels (I,K). In *Pn-1*-deficient cerebellum, the p27-negative oEGL is approximately twice the width of the iEGL (J,L). (**M**,**N**) Sections from P10 wild-type and *Pn-1*-deficient mice injected with BrdU 1 hour prior to sacrifice were immunostained (BrdU, green; Hoechst, blue). Analysis of the wild-type oEGL (M) reveals regularly dispersed BrdU-positive CGNPs (arrowheads), whereas the proliferating CGNPs of *Pn-1*-deficient mice are closer to the external pial border (N). (**O**) The ratio of BrdU positive versus negative CGNPs is not significantly altered in mutants. (**P**) Mutant mice show a significant decrease in the fraction of p27-labelled CGNPs. *P<0.05 (Student's t-test). (**Q**,**R**) P10 cerebellar sections of *Pn-1*$^{+/+}$ and *Pn-1*$^{-/-}$ mice immunostained for GFAP were analyzed by confocal microscopy. *Pn-1*$^{-/-}$ Bergmann glia display higher GFAP levels together with an increased thickness of and larger endfeet (R) in comparison to wild type (Q). iEGL, inner external granular layer; oEGL, outer external granular layer. Scale bars: 80 μm in B for A-D; 20 μm in F for E-H; 40 μm in I for I-J and in Q for Q,R; 15 μm in K for K-N and in inset in Q doe insets in Q,R.

cells were pre-treated with SHH for 5 hours prior to PN-1 addition (Fig. 3B). Pre-treatment with SHH did not significantly alter the inhibitory potential of PN-1, pointing to PN-1 having antagonistic effects on SHH signal transduction rather than on its direct competition for receptor binding.

Following this result, we also assessed the potential effects of PN-1 on cyclin D1, a known SHH target gene (Kenney and Rowitch, 2000). Indeed, cyclin D1 was detected at a high level in cells treated with SHH alone, and levels were lower by treatment with SHH and PN-1 (Fig. 3C). These results are consistent with the observed reduction in cell proliferation (compare Fig. 3C with Fig. 3A,B). Interestingly, cyclin D1 was also downregulated in cells treated with both SHH and RAP, thus indicating a possible requirement of LRPs for SHH-mediated stimulation of cell proliferation. The specificity of the antagonistic effects of PN-1 on SHH signal transduction was validated further by monitoring its ability to interfere with SHH-induced transcriptional activation. *Gli1* transcription was used as a sensitive read-out of SHH pathway activity in CGNPs cultured for 48 hours in the presence of SHH alone or with PN-1 (Fig. 3D). Whereas SHH alone upregulated *Gli1* expression, the addition of PN-1 reduced *Gli1* transcription to basal levels, as revealed by semi-quantitative reverse transcriptase (RT)-PCR analysis (Fig. 3D). To substantiate these results further, NIH3T3 cells, which are routinely used to assess SHH signal transduction (Yao et al., 2006), were transfected with a *Gli1* reporter plasmid (Dai et al., 1999). Treatment of transfected cells with SHH alone caused an approximately fourfold increase in the expression of the *Gli1* reporter gene within 24 hours, which could be blocked by PN-1 (Fig. 3E). Taken together, these results indicate that PN-1 antagonizes SHH signal transduction and/or the upregulation of the transcriptional target *Gli1*.

Next, the proliferation rates of mixed CGNPs/glial cells (Fig. 3F) and enriched CGNPs cultures (data not shown) isolated from wild-type and *Pn-1*-deficient mice were determined in response to SHH signalling. Indeed, mixed CGNP cultures from *Pn-1*$^{-/-}$ mice displayed an almost twofold-higher basal proliferation rate and a higher sensitivity to SHH-induced stimulation of proliferation than wild-type controls. Addition of PN-1 antagonized SHH-induced proliferation of both mutant and wild-type cells (Fig. 3F). In particular, the addition of 210 nM of recombinant PN-1 reduced the proliferation of *Pn-1*-deficient CGNP cultures to wild-type levels (Fig. 3F). The naturally occurring chemical cyclopamine (Cp), which blocks SHH signal reception, had little effect on the proliferation of wild-type cells, but reduced the proliferation of *Pn-1*-deficient cultures to wild-type levels (Fig. 3F). Enriched

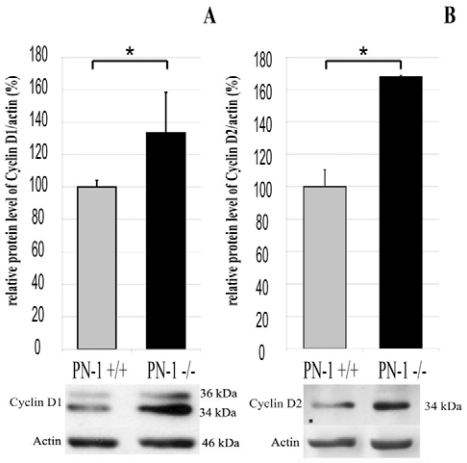

Fig. 6. *Pn-1*-deficient mice express higher levels of cyclin D1 and cyclin D2 in their cerebella. Cerebellum cortices of P10 *Pn-1*$^{+/+}$ and *Pn-1*$^{-/-}$ mice were homogenized and processed for immunoblot analysis. After densitometric quantification, the protein levels were monitored relatively to beta-actin and normalized to the *Pn-1*$^{+/+}$ value. Both cyclin D1 (**A**) and cyclin D2 (**B**) levels are increased in the mutant cerebellum. Values shown represent mean±s.e.m. **P*<0.05 (Student's *t*-test).

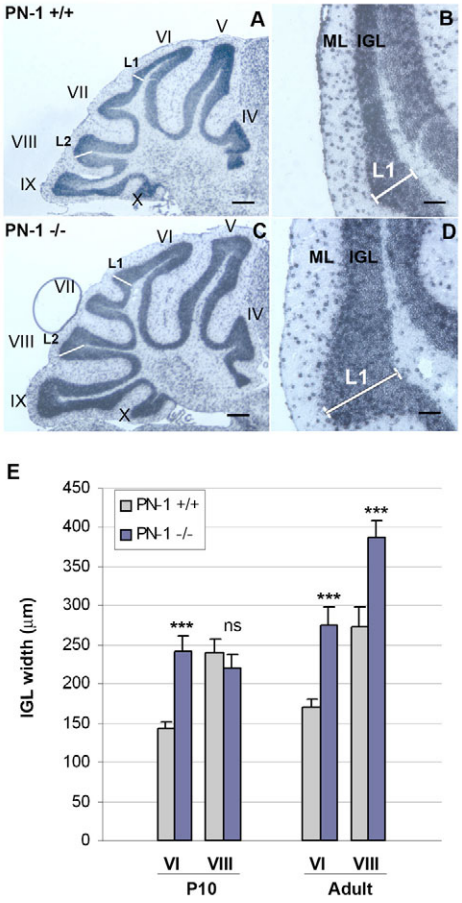

Fig. 7. PN-1 deficiency results in localized cerebellar expansion. Wild-type (**A**,**B**) and mutant (**C**,**D**) adult-cerebellar midsagittal sections were stained for *Ptc1* mRNA by in situ hybridization to reveal the IGL. The mutant cerebella show a global enlargement of the IGL in the zones facing the external side of the cerebellum. (B,D) Higher magnifications of lobe VI. (**E**) The thickness of the IGL was quantified measuring the highest widths in lobes VI and VIII (indicated as L1 and L2 in A-D). At P10, mutant cerebella exhibit a thicker IGL specifically in lobe VI (+67% compared to wild type). In the adults, this phenotype is still apparent (+60%). The thickness of lobe VIII is also increased, but to a lesser extent (+41%). IGL, internal granular layer; ML, molecular layer. (*n*=4 for P10; *n*=5 for adult; *** *P*<0.001; two-ways ANOVA test.) Scale bars: 300 μm in A,C; 100 μm in B,D.

CGNP cultures from *Pn-1*-deficient mice showed only a 28% increase in proliferation compared with the control (data not shown). This confirms that the glial population is the main source of PN-1 (also see Fig. S2 in the supplementary material) and provides evidence that the increased proliferation rates of *Pn-1*-deficient CGNP cultures could be due to overactivation of SHH signal transduction. These results indicate that PN-1 acts as a negative modulator of SHH signal transduction. Indeed, PN-1 inhibited SHH-induced differentiation of Bergmann glial cells (see Fig. S3 in the supplementary material). Taken together, these results show that PN-1 can antagonize both proliferation- and differentiation-inductive properties of SHH in culture.

Pn-1 deficiency potentiates the expression of SHH target genes in vivo

Given the higher SHH sensitivity of cultured *Pn-1*-deficient CGNPs, SHH signal transduction may be altered in *Pn-1*-deficient mice. Therefore, the expression of several SHH target genes was evaluated by in situ hybridization at P8 (Fig. 4 and see Fig. S4 in the supplementary material). *Gli1* and *Ptc1* are positive SHH targets and provide a sensitive read-out of SHH activity (Goodrich and Scott, 1998; Lee et al., 1997). Both genes were expressed in the EGL and by Bergmann glia in wild-type mice (Fig. 4A,C,G,H,J). In *Pn-1*$^{-/-}$ mice, the expression of both *Gli1* and *Ptc1* was increased in cells within the outer EGL (oEGL) [Fig. 4B,D,I,K; identified as MATH1 (also known as anti-ATOH1)-positive CGNPs: see Fig. 5F]. In addition, higher levels of *Gli1* and *Ptc1* expression were also detected in Bergmann glia in *Pn-1*-deficient mice (see Fig. S4 in the supplementary material).

Shh and *Gli3* are expressed in rather complementary patterns and have been shown to functionally antagonize one another (Zeller, 2004). *Gli3* was broadly expressed in the EGL and in the internal granular layer (IGL) of wild-type mice (Fig. 4E,L), whereas its expression was lower and more-restricted in *Pn-1*-deficient mice (Fig. 4F,M). Interestingly, *Gli3* expression was normal in the external part of the cerebellum but significantly reduced in fissures (Fig. 4F). The changes are not due to altering *Shh* itself, because *Shh* was expressed at similar levels in both wild-type and mutant mice (predominantly in Purkinje cells; Fig. 4N,O). The results were confirmed by semi-quantitative RT-PCR analysis, which revealed that the expressions of *Gli1* and *Ptc1* were significantly increased while that of *Gli3* was reduced in the cerebellum of *Pn-1*-deficient mice (see Fig. S5 in the supplementary material). Taken together, these studies corroborate the proposal that SHH signal transduction is potentiated in mice lacking *Pn-1*.

CGNP differentiation is delayed in *Pn-1*-deficient mice

In *Pn-1*-deficient mice, the overall thickness of the EGL was not altered at P5 and P10 (data not shown). By contrast, the *Pn-1* deficiency resulted in a thickening of the oEGL and thinning of the inner EGL (iEGL; Fig. 5A-L). The bHLH transcription factor

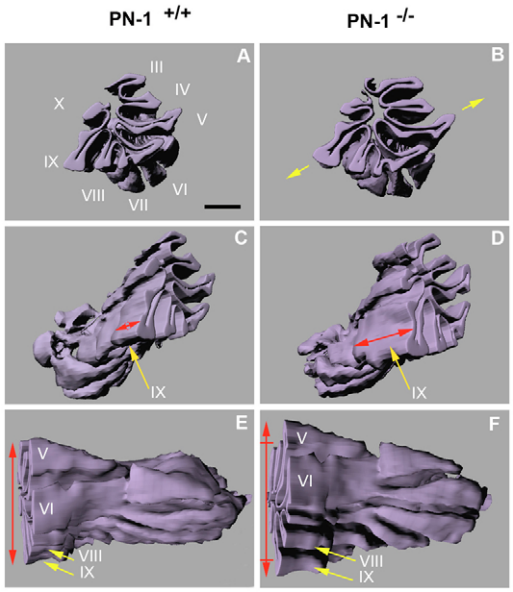

Fig. 8. 3-D reconstruction of representative wild-type and *Pn-1*-deficient adult cerebella. (**A-F**) Half-cerebella of two representative wild-type (*Pn-1*$^{+/+}$; A,C,E) and *Pn-1*-deficient mutant (B,D,F) mice are shown as 3-D reconstructions from different angles. (A,B) The cerebella shown as mid-sections. Notice that the overall size of the mutant cerebellum (B) is increased. In particular, lobes V and IX appear extended in the direction of the yellow arrows. (C,D) The cerebella shown from a posterior angle. In the mutant mouse, lobe IX (yellow arrow), again appears enlarged in its mid-part (red double arrows). (E,F) View from the mid-anterior side. The central part of the mutant cerebellum appears clearly enlarged (red double arrows) and lobe IX (yellow arrows) protrudes more than in its wild-type counterpart.

MATH1 identifies the early progenitors of the granular lineage (Ben Arie et al., 1997). The number of immature MATH1-positive CGNPs increased slightly at P5 (data not shown) and significantly at P10 in *Pn-1*-deficient mice (Fig. 5A-H), and MATH1 immunoreactivity was stronger in mutant CGNPs (Fig. 5E,F). To analyze the postmitotic zone of the EGL, the p27 cyclin-dependent kinase inhibitor, which accumulates in the nuclei of postmitotic CGNPs, was used to monitor differentiation (Miyazawa et al., 2000). In wild-type cerebella, overall p27 staining was weak in the oEGL and became more intense as CGNPs entered the iEGL (Fig. 5I,K). In *Pn-1*-deficient mice, the decrease in iEGL thickness was noticeable at P5 (data not shown) and obvious by P10 (Fig. 5J-L). The intensity of p27 staining was reduced in the expanded oEGL and was restricted to a limited region of the iEGL (Fig. 5L). In agreement, the ratio of p27-labelled to non-labelled cells was significantly reduced in *Pn-1*-deficient mice by P10 (Fig. 5P). This delay in CGNP differentiation was further evidenced by immunodetection of doublecortin, an early marker for neuronal differentiation (Gleeson et al., 1999), whose expression was decreased in *Pn-1*-deficient mice (see Fig. S6 in the supplementary material). These results show that the onset of differentiation is delayed in CGNPs of *Pn-1*-deficient mice. However, during the stages analyzed, this delay did not correlate with significantly altered proliferation rates (Fig. 5M-O and data not shown). Interestingly, the BrdU-labelled CGNPs remained located close to the pial surface in *Pn-1*$^{-/-}$ cerebella (Fig. 5N), whereas the proliferative CGNPs were spread throughout the oEGL in wild-type littermates (Fig. 5M, arrowheads). We also studied whether PN-1 modulates the SHH-mediated differentiation of Bergmann glial cells in vivo. Indeed, an overall increase in the thickness of GFAP-positive fibres was observed in Bergmann glial cells at P10 in *Pn-1*-deficient mice (Fig. 5R). The Bergmann glial fibres appeared irregular and contacted the pial surface with larger endfeet in comparison to wild-type (Fig. 5Q). These results indicate that the SHH-mediated effects on the proliferation of CGNPs and differentiation of Bergmann glia cells are potentiated *in Pn-1*-deficient mice. Finally, the in vivo levels of the cell cycle regulators cyclin D1 and cyclin D2, two SHH targets (Kenney and Rowitch, 2000), were evaluated. Immunoblot analysis was performed on cerebellar extracts from P10 wild-type and *Pn-1*-deficient mice. The levels of cyclin D1 and cyclin D2 were increased by 33 and 68%, respectively, in mutant cerebella (Fig. 6A,B).

Pn-1 deficiency induces cerebellar overgrowth

The differentiation impairments caused by *Pn-1* deficiency during postnatal development prompted us to evaluate the overall morphology of the cerebellum. The thickness of the IGL was examined in *Pn-1*$^{+/+}$ and *Pn-1*$^{-/-}$ mice at P5, P10 and in adults. The gross morphology of the P5 mutant cerebellum was similar to that of wild type (data not shown). By contrast, P10 mutant mice showed an increased thickness of the external IGL that was restricted to the anterior-central part of the cerebellum (see Fig. S7 in the supplementary material). In particular, the IGL of lobe VI showed a 67% increase in thickness compared with its wild-type counterpart (Fig. 7E). The IGL of the posterior lobes and zones facing the deep fissures were unaffected. The observed phenotype became more prominent in adult mutant mice (Fig. 7A-E); the width of the IGL in posterior lobe VIII showed a 40% increase and the IGL of lobe VI was 60% thicker in comparison to wild type. Thus, the *Pn-1* deficiency probably resulted in an overproduction of mature granular cells, which caused the enlarged IGL. However, this difference in thickness may not necessarily reflect differences in the total volume of the IGL, because there may be compensation. Therefore, both wild-type and mutant cerebella (P10 and adults) were serially reconstructed (Fig. 8). The complete IGL in the cerebellum of three pairs of age-matched wild-type and *Pn-1*-deficient mice was measured. At P10, the mutant cerebellum showed a 6% increase in volume in comparison to wild type (data not shown), whereas the overall increase was 12.2% in adults. Potential regional differences were assessed by subdividing the cerebellum into three regions: anterior (lobes III-V), medial (lobes VI-VII) and posterior lobes (lobes VIII-X). At P10, the medial part was most affected (data not shown). In the adult, the anterior, medial and posterior regions of *Pn-1*-deficient mice showed an increase of 11.3, 9.3 and 15.4%, respectively. Moreover, the 3-D reconstruction of wild-type and mutant cerebella revealed an elongation of the anterior and posterior parts in comparison to wild type (Fig. 8B-D,F, red double arrows,). In particular, lobe IX protruded much more in *Pn-1*-deficient mice (Fig. 8D). Interestingly, these enlarged and elongated territories contained the highest levels of PN-1 protein during early development (Fig. 1). Taken together, this in vivo analysis suggests a modulatory role of PN-1 during cerebellar development.

DISCUSSION

The present study establishes PN-1 as a modulator of neuronal precursor proliferation and differentiation in the postnatal developing cerebellum. *Pn-1* expression was high during the active phase of CGNP proliferation and was downregulated during differentiation. PN-1 inhibited SHH-induced CGNP proliferation

and CGNPs isolated from *Pn-1*-deficient mice displayed higher proliferation rates. In vivo, an increased number of CGNPs expressed *Gli1* and *Ptc1* in the oEGL of mutant mice. The cerebellar development of *Pn-1*-deficient mice resulted in an enlarged oEGL and a reduced iEGL. SHH-regulated maturation of the Bergmann glia was potentiated in *Pn-1-deficient* mice. In addition, the SHH targets cyclin D1 and cyclin D2 were overexpressed in mutant cerebellum. Finally, the *Pn-1* gene deficiency caused a regionalized increase of the IGL, which led to a localized size increase in the adult cerebellum. Thus, PN-1 functions in combination with SHH to shape the adult cerebellum. SHH binds Megalin (also known as gp330 and LRP2) with high affinity and is endocytosed via LRP family members (McCarthy et al., 2002). Nybakken and Perrimon (Nybakken and Perrimon, 2002) proposed that the SHH-LRP interaction may allow the clustering of PTC1, SMO and SHH, thus causing internalization and potentiation of the signal. However, the biological relevance of LRP in SHH signal transduction remained unclear. Using RAP, we provide evidence that LRP accessibility is important for SHH-mediated stimulation of CGNP proliferation. Proteoglycans are crucial for binding to LRP and for the subsequent internalization of ligands, such as PN-1 (Crisp et al., 2000). Interestingly, proteoglycans are also required for SHH-induced proliferation of progenitor cells in the postnatal developing cerebellum (Rubin et al., 2002). Because PN-1 is known to bind to several LRP family members (Croy et al., 2003), it is possible that PN-1 and SHH could share the same LRP receptors on CGNPs. In agreement with other studies, we demonstrate that PN-1 uptake is mediated by LRP1. Moreover, microarray analysis indicates that, in the cerebellum, *LRP1* transcripts are at least tenfold more abundant than any other LRPs (data not shown). Thus, LRP1 seems to be the best candidate for mediating the PN-1 and SHH interactions during CGNP proliferation. The potential competition for LRP-binding sites may be mechanistically similar to what has been reported for dickkopf 1 (DKK1) and the Wnt modulator Wise (also known as SOSTDC1 – Mouse Genome Informatics), which inhibit Wnt signalling by interacting with LRP5 and/or LRP6 (Glinka et al., 1998). However, we cannot exclude that the interaction of PN-1 with LRPs also interferes with other ligands sharing this co-receptor, such as BMP4. In fact, BMP4 is present in the EGL (Rios et al., 2004) and interacts with LRP2, which induces its clearance (Spoelgen et al., 2005).

The cerebella phenotype of *Pn-1*-deficient mice corroborates the results obtained by the analysis of primary CGNP cultures. The *Pn-1* deficiency results in increased expression of the SHH transcriptional targets *Gli1* and *Ptc1* in the oEGL, indicative of enhanced SHH signal transduction. Furthermore, the number of immature CGNPs and the initiation of their differentiation is enhanced in mutant mice, which is detrimental to the postmitotic iEGL. These changes in CGNP differentiation probably underlie the enlargement of the IGL from P10 onwards. The increase in IGL thickness follows an anteroposterior gradient: it initiates in lobe VI and affects more-posterior lobes as differentiation progresses. It is interesting to note that these regions correspond to the territories with the highest PN-1 protein levels during cerebellar development. Studies using gain- and loss-of-function approaches have established that the SHH-mediated, controlled local increase in the proliferation of CGNPs determines the extent of cerebellar foliation (Corrales et al., 2004; Corrales et al., 2006; Lewis et al., 2004). These authors postulate that regulation of the length and intensity of SHH signalling is crucial to lobule formation. We now identify the PN-1 extracellular serine protease inhibitor as a valuable candidate modulator. Indeed, SHH overexpression in transgenic mice does not alter EGL thickness or CGNP proliferation in the oEGL between P5 and P10, but the IGL is expanded from P8 onwards (Corrales et al., 2004; Corrales et al., 2006). In adult transgenic mice, all cerebellar lobes exhibit a thickened IGL as also observed in *Pn-1*-deficient mice. Our study uncovers a role of PN-1 in the cellular events that are controlled by morphogenetic SHH signalling during cerebellar development. PN-1 may restrain SHH-mediated proliferation and thereby contribute to the regulation of the size and shape of the cerebellum via the fine-tuning of SHH-mediated foliation. This would explain the rather localized gross-morphological phenotype observed in *Pn-1*-deficient mice. Further investigation is necessary to understand how PN-1 may participate in the formation and maintenance of an anteroposterior gradient of SHH signal transduction, and how PN-1 may potentially impact the switch from proliferation to differentiation.

We are grateful to S. Arber and N. Hynes for critical reading of the manuscript. We also thank U. Mueller, S. Pons, S. Ishii, M. Etzerodt, D. Strickland, J. Johnson and A. Zuniga for comments and reagents. We thank A. Weigel, M. Lino, F. Fischer and P. Schwarb for valuable technical assistance. This work was supported by the Novartis Research Foundation (to D.M.) and the Swiss National Science Foundation (to R.Z.).

Supplementary material

Supplementary material for this article is available at
http://dev.biologists.org/cgi/content/full/134/9/1745/DC1

References

Baker, J. B., Low, D. A., Simmer, R. L. and Cunningham, D. D. (1980). Protease-nexin: a cellular component that links thrombin and plasminogen activator and mediates their binding to cells. *Cell* **21**, 37-45.

Ben Arie, N., Bellen, H. J., Armstrong, D. L., McCall, A. E., Gordadze, P. R., Guo, Q., Matzuk, M. M. and Zoghbi, H. Y. (1997). Math1 is essential for genesis of cerebellar granule neurons. *Nature* **390**, 169-172.

Corrales, J. D., Rocco, G. L., Blaess, S., Guo, Q. and Joyner, A. L. (2004). Spatial pattern of sonic hedgehog signaling through Gli genes during cerebellum development. *Development* **131**, 5581-5590.

Corrales, J. D., Blaess, S., Mahoney, E. M. and Joyner, A. L. (2006). The level of sonic hedgehog signaling regulates the complexity of cerebellar foliation. *Development* **133**, 1811-1821.

Crisp, R. J., Knauer, D. J. and Knauer, M. F. (2000). Roles of the heparin and low density lipid receptor-related protein-binding sites of protease nexin 1 (PN1) in urokinase-PN1 complex catabolism. The PN1 heparin-binding site mediates complex retention and degradation but not cell surface binding or internalization. *J. Biol. Chem.* **275**, 19628-19637.

Croy, J. E., Shin, W. D., Knauer, M. F., Knauer, D. J. and Komives, E. A. (2003). All three LDL receptor homology regions of the LDL receptor-related protein bind multiple ligands. *Biochemistry* **42**, 13049-13057.

Dahmane, N. and Altaba, A. (1999). Sonic hedgehog regulates the growth and patterning of the cerebellum. *Development* **126**, 3089-3100.

Dai, P., Akimaru, H., Tanaka, Y., Maekawa, T., Nakafuku, M. and Ishii, S. (1999). Sonic Hedgehog-induced activation of the Gli1 promoter is mediated by GLI3. *J. Biol. Chem.* **274**, 8143-8152.

Easwaran, V., Lee, S. H., Inge, L., Guo, L., Goldbeck, C., Garrett, E., Wiesmann, M., Garcia, P. D., Fuller, J. H., Chan, V. et al. (2003). beta-Catenin regulates vascular endothelial growth factor expression in colon cancer. *Cancer Res.* **63**, 3145-3153.

Gleeson, J. G., Lin, P. T., Flanagan, L. A. and Walsh, C. A. (1999). Doublecortin is a microtubule-associated protein and is expressed widely by migrating neurons. *Neuron* **23**, 257-271.

Glinka, A., Wu, W., Delius, H., Monaghan, A. P., Blumenstock, C. and Niehours, C. (1998). Dickkopf-1 is a member of a new family of secreted proteins and functions in head induction. *Nature* **391**, 357-362.

Gloor, S., Odink, K., Guenther, J., Nick, H. and Monard, D. (1986). A glia-derived neurite promoting factor with protease inhibitory activity belongs to the protease nexins. *Cell* **47**, 687-693.

Goodrich, L. V. and Scott, M. P. (1998). Hedgehog and patched in neural development and disease. *Neuron* **21**, 1243-1257.

Hatten, M. E. (1985). Neuronal regulation of astroglial morphology and proliferation in vitro. *J. Cell Biol.* **100**, 384-396.

Hatten, M. E., Lynch, M., Rydel, R. E., Sanchez, J., Joseph-Silverstein, J., Moscatelli, D. and Rifkin, D. B. (1988). In vitro neurite extension by granule neurons is dependent upon astroglial-derived fibroblast growth factor. *Dev. Biol.* **125**, 280-289.

Herz, J., Goldstein, J. L., Strickland, D. K., Ho, Y. K. and Brown, M. S. (1991).

39-kDa protein modulates binding of ligands to low density lipoprotein receptor-related protein/alpha 2-macroglobulin receptor. *J. Biol. Chem.* **266**, 21232-21238.
Ho, K. S. and Scott, M. P. (2002). Sonic hedgehog in the nervous system: functions, modifications and mechanisms. *Curr. Opin. Neurobiol.* **12**, 57-63.
Ingham, P. W. and McMahon, A. P. (2001). Hedgehog signaling in animal development: paradigms and principles. *Genes Dev.* **15**, 3059-3087.
Kenney, A. M. and Rowitch, D. H. (2000). Sonic hedgehog promotes G(1) cyclin expression and sustained cell cycle progression in mammalian neuronal precursors. *Mol. Cell. Biol.* **20**, 9055-9067.
Klein, R. S., Rubin, J. B., Gibson, H. D., DeHaan, E. N., Alvarez-Hernandez, X., Segal, R. A. and Luster, A. D. (2001). SDF-1 alpha induces chemotaxis and enhances Sonic hedgehog-induced proliferation of cerebellar granule cells. *Development* **128**, 1971-1981.
Knauer, D. J., Majumdar, D., Fong, P. C. and Knauer, M. F. (2000). SERPIN regulation of factor XIa. The novel observation that protease nexin 1 in the presence of heparin is a more potent inhibitor of factor XIa than C1 inhibitor. *J. Biol. Chem.* **275**, 37340-37346.
Knauer, M. F., Hawley, S. B. and Knauer, D. J. (1997a). Identification of a binding site in protease nexin I (PN1) required for the receptor mediated internalization of PN1-thrombin complexes. *J. Biol. Chem.* **272**, 12261-12264.
Knauer, M. F., Kridel, S. J., Hawley, S. B. and Knauer, D. J. (1997b). The efficient catabolism of thrombin-protease nexin 1 complexes is a synergistic mechanism that requires both the LDL receptor-related protein and cell surface heparins. *J. Biol. Chem.* **272**, 29039-29045.
Kury, P., Schaeren-Wiemers, N. and Monard, D. (1997). Protease nexin-1 is expressed at the mouse met-/mesencephalic junction and FGF signaling regulates its promoter activity in primary met-/mesencephalic cells. *Development* **124**, 1251-1262.
Kvajo, M., Albrecht, H., Meins, M., Hengst, U., Troncoso, E., Lefort, S., Kiss, J. Z., Petersen, C. C. and Monard, D. (2004). Regulation of brain proteolytic activity is necessary for the in vivo function of NMDA receptors. *J. Neurosci.* **24**, 9734-9743.
Lee, A., Kessler, J. D., Read, T. A., Kaiser, C., Corbeil, D., Huttner, W. B., Johnson, J. E. and Wechsler-Reya, R. J. (2005). Isolation of neural stem cells from the postnatal cerebellum. *Nat. Neurosci.* **8**, 723-729.
Lee, J., Platt, K. A., Censullo, P. and Altaba, A. (1997). Gli1 is a target of Sonic hedgehog that induces ventral neural tube development. *Development* **124**, 2537-2552.
Lewis, P. M., Gritli-Linde, A., Smeyne, R., Kottmann, A. and McMahon, A. P. (2004). Sonic hedgehog signaling is required for expansion of granule neuron precursors and patterning of the mouse cerebellum. *Dev. Biol.* **270**, 393-410.
Luthi, A., Van der Putten, H., Botteri, F. M., Mansuy, I. M., Meins, M., Frey, U., Sansig, G., Portet, C., Schmutz, M., Schroder, M. et al. (1997). Endogenous serine protease inhibitor modulates epileptic activity and hippocampal long-term potentiation. *J. Neurosci.* **17**, 4688-4699.
Mansuy, I. M., Van der Putten, H., Schmid, P., Meins, M., Botteri, F. M. and Monard, D. (1993). Variable and multiple expression of Protease Nexin-1 during mouse organogenesis and nervous system development. *Development* **119**, 1119-1134.
McCarthy, R. A., Barth, J. L., Chintalapudi, M. R., Knaak, C. and Argraves, W. S. (2002). Megalin functions as an endocytic sonic hedgehog receptor. *J. Biol. Chem.* **277**, 25660-25667.
Meier, R., Spreyer, P., Ortmann, R., Harel, A. and Monard, D. (1989). Induction of glia-derived nexin after lesion of a peripheral nerve. *Nature* **342**, 548-550.
Michos, O., Panman, L., Vintersten, K., Beier, K., Zeller, R. and Zuniga, A. (2004). Gremlin-mediated BMP antagonism induces the epithelial-mesenchymal feedback signaling controlling metanephric kidney and limb organogenesis. *Development* **131**, 3401-3410.
Miyazawa, K., Himi, T., Garcia, V., Yamagishi, H., Sato, S. and Ishizaki, Y. (2000). A role for p27/Kip1 in the control of cerebellar granule cell precursor proliferation. *J. Neurosci.* **20**, 5756-5763.
Nicot, A., Lelievre, V., Tam, J., Waschek, J. A. and DiCicco-Bloom, E. (2002). Pituitary adenylate cyclase-activating polypeptide and sonic hedgehog interact to control cerebellar granule precursor cell proliferation. *J. Neurosci.* **22**, 9244-9254.
Nybakken, K. and Perrimon, N. (2002). Hedgehog signal transduction: recent findings. *Curr. Opin. Genet. Dev.* **12**, 503-511.
Pons, S., Trejo, J. L., Martinez-Morales, J. R. and Marti, E. (2001). Vitronectin regulates Sonic hedgehog activity during cerebellum development through CREB phosphorylation. *Development* **128**, 1481-1492.
Rios, I., Alvarez-Rodriguez, R., Marti, E. and Pons, S. (2004). Bmp2 antagonizes sonic hedgehog-mediated proliferation of cerebellar granule neurones through Smad5 signalling. *Development* **131**, 3159-3168.
Rubin, J. B., Choi, Y. and Segal, R. A. (2002). Cerebellar proteoglycans regulate sonic hedgehog responses during development. *Development* **129**, 2223-2232.
Schneider, W. J. and Nimpf, J. (2003). LDL receptor relatives at the crossroad of endocytosis and signaling. *Cell Mol. Life Sci.* **60**, 892-903.
Sommer, J., Meyhack, B., Rovelli, G., Buergi, R. and Monard, D. (1989). Synthesis of glia-derived nexin in yeast. *Gene* **85**, 453-459.
Spoelgen, R., Hammes, A., Anzenberger, U., Zechner, D., Andersen, O. M., Jerchow, B. and Willnow, T. E. (2005). LRP2/megalin is required for patterning of the ventral telencephalon. *Development* **132**, 405-414.
Strickland, D. K. and Ranganathan, S. (2003). Diverse role of LDL receptor-related protein in the clearance of proteases and in signaling. *J. Thromb. Haemost.* **1**, 1663-1670.
Wallace, V. A. (1999). Purkinje-cell-derived Sonic hedgehog regulates granule neuron precursor cell proliferation in the developing mouse cerebellum. *Curr. Biol.* **9**, 445-448.
Wechsler-Reya, R. J. and Scott, M. P. (1999). Control of neuronal precursor proliferation in the cerebellum by Sonic Hedgehog. *Neuron* **22**, 103-114.
Yao, S., Lum, L. and Beachy, P. (2006). The ihog cell-surface proteins bind Hedgehog and mediate pathway activation. *Cell* **125**, 343-357.
Zeller, R. (2004). It takes time to make a pinky: unexpected insights into how SHH patterns vertebrate digits. *Sci. STKE* **2004**, e53.